MethodsX 10 (2023) 102025

Contents lists available at ScienceDirect

MethodsX

journal homepage: www.elsevier.com/locate/mex

Method Article

# Two-photon polymerization based reusable master template to fabricate polymer microneedles for drug delivery

Mamatha M. Pillai, Saranya Ajesh, Prakriti Tayalia*

*Department of Biosciences and Bioengineering, Indian Institute of Technology Bombay, India*

ARTICLE INFO

*Method name:*
Two photon polymerization

*Keywords:*
2PP
Microneedle template
Annealing
PDMS molds
PVA microneedle patch

ABSTRACT

Microneedle patches have been widely used in a minimally invasive manner for various drug delivery applications. However, for developing these microneedle patches, master molds are required, which are generally made of metal and are very expensive. Two-photon polymerization (2PP) technique can be used for fabricating microneedles more precisely and at a much lower cost. This study reports a novel strategy for developing microneedle master templates using the 2PP method. The main advantage of this technique is that there is no requirement for post-processing after laser writing, and that for the fabrication of polydimethylsiloxane (PDMS) molds, harsh chemical treatments such as silanization are not required. This is a one-step process for manufacturing of microneedle templates which allows easy replication of negative PDMS molds. This is done by adding resin to the master-template and annealing at a specific temperature, thereby making the PDMS peel-off easy and allowing re-use of the master template multiple times. Using this PDMS mold, two types of polyvinyl alcohol (PVA)-rhodamine (RD) microneedle patches were developed, namely, dissolving (D-PVA) and hydrogel (H-PVA) patches and were characterized using suitable techniques. This technique is affordable, efficient and does not require post-processing for development of microneedle templates required for drug delivery applications.

- Two photon polymerization can be used for cost-effective fabrication of polymer microneedles for transdermal drug delivery.
- Post-processing or surface-modification procedures are not required for these master templates.
- Using a simple annealing step, the master template becomes reusable and robust for peeling off polymers like PDMS.

## Specifications Table

| | |
|---|---|
| Subject area: | Materials Science |
| More specific subject area: | Biotechnology and Bioengineering |
| Name of your method: | Two photon polymerization |
| Name and reference of original method: | Not applicable |
| Resource availability: | Not applicable |

* Corresponding author.
*E-mail address:* prakriti@iitb.ac.in (P. Tayalia).

https://doi.org/10.1016/j.mex.2023.102025
Received 4 October 2022; Accepted 17 January 2023
Available online 22 January 2023
2215-0161/© 2023 The Authors. Published by Elsevier B.V. This is an open access article under the CC BY-NC-ND license (http://creativecommons.org/licenses/by-nc-nd/4.0/)

## Background

Medicated transdermal formulations have been attractive, suitable and affordable for treating many disease conditions. Drug release from such topical ointments or dermal patches leads to absorption by the stratum corneum or diffusion through the epidermis and uptake by the dermal papillary layers. However, this method has low drug diffusivity through the skin barriers [1]. Patches with a tiny array of microneedles loaded with therapeutic agents can overcome these limitations and enhance the effectiveness of drug permeation through the skin. These microneedles can deliver therapeutics by piercing the epidermis and dermis, thereby bypassing the barrier layers. Microneedles can also be used to deliver specific genes to activate the immune mechanisms of the body to fight against disease conditions. Microneedle patches are semi-invasive and relatively painless for administering drugs or medicated formulations [2]. A plethora of biocompatible and biodegradable polymers and their composites have been used for the fabrication of microneedle patches. Polymer microneedle patches are particularly useful because of their affordability and versatility in terms of the development of a varied range of microneedle shapes, such as solid, hollow, tapered-end, or cylindrical needles of desired length and arrays. Different polymers such as polyvinyl alcohol (PVA), polyvinylpyrrolidone, starch, cellulose, chitosan, and sodium alginate have been used to develop dissolving, hollow, or solid microneedles for the delivery of drugs. However, preparation of a robust master template is a prerequisite for the fabrication of polymer microneedles. From these master templates, PDMS-negative or positive molds are made for casting the desired polymers with drug formulations and fabricating the microneedles [3]. These master templates can be prepared from silicon or glass but are very expensive and fragile. Metal-based master templates are fabricated using laser cutting techniques that are quite expensive and require expensive facilities and skilled personnel. 3D printing techniques such as fused deposition modelling using polymer filaments such as acrylonitrile butadiene styrene (ABS) and polylactic acid (PLA) can be used. Although this method is cost-effective, the resolution that can be achieved is limited and allows printing only micron-scale features [4,5]. Two-photon polymerization is an advanced technique used for printing nano- as well as micron-scale features with high precision. Polymers or resins can be photopolymerized into any desired structure using a femtosecond laser beam. The advantages of this technique are that different sizes and shapes of needles can be printed with high aspect ratio, high resolution, precision, and reproducibility in a cost-effective manner [6].

Typically, the microneedle master templates fabricated using 2PP require multiple processing steps to develop polymer microneedles. After printing the master template, PDMS cannot be cast directly on the structures because the elastomer adheres to the template during the curing and de-molding process [4]. To prevent this, the surface of the master template is treated with hazardous chemicals such as trichloro (1H, 1H, 2H, 2H-perfluorooctyl) silane or perfluorodecyltrichlorosilane [4]. Further, since these master templates comprise high aspect ratio microneedle structures required for drug delivery applications, they need to be robust to prevent their breaking during the process of PDMS molding. In this study, we have optimised a novel one-step approach that requires less than 6 min of processing time after the master template is fabricated. Further, it allows multiple replications of PDMS molds without distorting the microneedle array or breaking the master template. The microneedle master templates created using 2PP were spin-coated with the photoresist and annealed at high temperature. To our knowledge, this is the first report on a temperature-based annealing technique that can be implemented for 2PP written microneedle master templates. Main advantage of this process is that PDMS can be directly cast on the templates without any additional surface treatments and can be removed without distorting or breaking the template. Using this method, we have fabricated two types of microneedle patches: the dissolving (D-PVA) and hydrogel (H-PVA) microneedle patches. Rhodamine B was incorporated as a model drug to study the release profile. Furthermore, physical and biological characterization of these microneedle patches was performed to validate the potential of our technique. This strategy for the development of polymer microneedle patches is cost-effective and scalable.

## Method details

### *Designing the template*

The microneedle array was designed in Solidworks software and imported as a .stl file in Nanoscribe software. This created a .gwl job file, which was loaded into the Describe software for optimization of printing parameters and total hours of laser writing required for fabricating a particular template.

### *Fabrication of template using 2PP*

The master template design was imported to a Nanoscribe Photonic Professional GT (Nanoscribe, Germany) for direct laser writing or 2PP. The substrate used for 2PP was indium tin oxide (ITO) coated glass slide (Nanoscribe, Germany). A drop of IPS resin (Nanoscribe, Germany) was placed on the surface of the ITO coated glass slide. For laser writing, a 25x objective with a numerical aperture of 0.8 was used for focusing the laser beam. The desired structure was written on the glass slide in a layer-by-layer fashion and monitored using a real-time camera. After completion of the writing process, another drop of resin was added on top of the master template and spin-coated at 6000 rpm for 2 min and annealed at 190 °C for 3 min. An unannealed structure was also fabricated for comparison.

### *Preparation of microneedle array molds*

PDMS molds were cast out of the 2PP written templates. For this PDMS pre-polymer mix was prepared by mixing the base and curing agent (10:1) and kept in a vacuum desiccator for 30 min for removal of gas bubbles. This PDMS pre-polymer mix was poured

**Table 1**
Dimensions of microneedle master template.

| PARAMETERS | DIMENSIONS |
|---|---|
| Needle height | 800 μm |
| Needle base diameter | 250 μm |
| Needle tip diameter | 30 μm |
| Distance between needles | 1 mm |
| Base height | 50 μm |
| Array size | 3 × 3 |
| Total area of template | 4 × 4 mm |

onto the microneedle master template and again degassed using a vacuum desiccator. The master template with PDMS pre-polymer was cured at 70 °C for 2 h in a vacuum oven and then allowed to cool at room temperature. The PDMS mold was peeled off slowly from the master template and used as a negative mold for fabrication of polymer microneedle arrays.

*Development of polymer microneedles*

Polyvinyl alcohol (PVA) (10% w/v) was used for making microneedle patches. PVA was dissolved in distilled water and crosslinked using a green crosslinker, citric acid (2% w/v). Rhodamine B was used as a model drug and incorporated (1 mg/ml) into the PVA solution. This polymer mix was cast on the PDMS mold, degassed using a vacuum desiccator for 10 min, and then centrifuged at 3000 rpm for 15 min at room temperature. This was repeated twice and then kept for drying overnight in a vacuum oven at 40 °C. The microneedle patch was then peeled off and used for further characterization. PVA microneedle patch without any crosslinker was also developed using a similar method. Thus, the two different microneedle patches were as follows: dissolving microneedles (D-PVA) without the cross-linker and the hydrogel microneedles (H-PVA) with the cross-linker.

*Characterization of microneedles*

For visual characterization, the master template and polymer microneedle patches were imaged using a stereomicroscope (SMZ 18, Nikon) as well as a scanning electron microscope (SEM). Confocal images (LSM780, Carl Zeiss) of rhodamine-incorporated polymer microneedle patches were also taken. Crosslinked microneedles were subjected to swelling in PBS solution for 24 h and stereo microscopy images were taken before and after swelling. A cumulative release profile of rhodamine from crosslinked PVA microneedles was assessed. For this, a known concentration of the model drug was loaded into the microneedle patch and cast in the PDMS mold. Patches were kept in PBS and at different time intervals, PBS was removed for analysis and fresh PBS was replenished. To determine the concentration of rhodamine that was released, fluorescence of collected PBS samples was taken at 546 nm. A standard curve at different concentrations of rhodamine was used to calculate the unknown concentration released at different time points. In vitro degradation study was performed using simulated body fluids (SBF) (ASTM F1635-04) [7]. For this microneedle patches were soaked in SBF solution and at different time points, samples were dried and weight was measured. The percentage of weight retained was calculated as per the following equation:

$$Weight(\%) = (Wi - Wf)/Wi \; x \; 100$$

where Wi is the initial weight and Wf is the final weight of the patches.

A universal testing machine (UTM) was used to perform compression test for examining the mechanical characteristics of the microneedles. For the analysis, a 3 × 3 array of the microneedle patch was used. Microneedles were compressed upto a height of 600 μm and stress vs. strain graph corresponding to this compression was plotted.

*Skin penetration analysis using computer simulation*

The simulations were performed using COMSOL Multiphysics version 5.5. Skin was represented by three layers, namely the stratum corneum (10 μm thickness), epidermis (150 μm) and dermis (1000 μm) [8], which had Young's moduli of 26 MPa, 0.136 MPa, and 0.066 MPa, respectively and a Poisson's ratio of 0.49 [9,10]. Microneedles were modelled as per the dimensions given in Table 1. Different shapes such as cylindrical, pyramidal, and serrated microneedles were used to compare their stress profiles. Studies have shown that skin is resistant to penetration upon application of an axial load of 3.18 MPa at the needle tip [11]. Young's modulus of microneedles was estimated via compression test, and the same was fed into the model for simulation. Simulations were performed for single as well as an array of microneedles.

*Hemocompatibility analysis*

The effect of PVA microneedle patches on erythrocytes was determined by performing hemocompatibility analysis as per ASTM F756-00 (2000) standard [8]. Microneedle patches were directly incubated with blood diluted in PBS (10:1 ratio) for 1 h at 37 °C. RBC lysis buffer was used to completely lyse the blood, which was used as a positive control while only PBS with the patch was

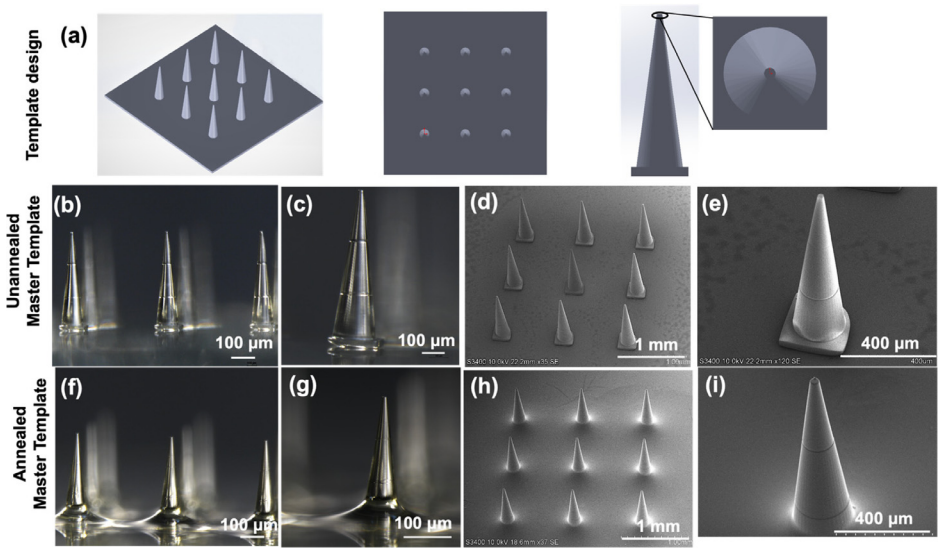


**Fig. 1.** (a) Microneedle template design; (b-c) stereomicroscopic images and, (d-e) SEM images of unannealed master template; (f-g) stereomicroscopic images, and (h-i) SEM images of annealed master template.

used as blank. After 1 h of incubation, samples were centrifuged at 2500 rpm for 5 min and supernatant was used to measure the absorbance at 540 nm. The hemolytic index was calculated as reported in Pillai et al. [12] using the following equation:

$$Hemolysis(\%) = \left[(OD\ of\ Sample - OD\ of\ Negative\ Control)/OD\ of\ Positive\ Control\right]\ x\ 100$$

*In vitro cytocompatibility assay*

For evaluating the cytocompatibility of polymer microneedles, human adult dermal fibroblast (HADF) cells were cultured in a 96-well plate and direct contact assay was performed as per the ISO 10993-5 guidelines [13]. Briefly, 1 × 105 HADF cells/well were cultured in a 96-well plate for 24 h after which 6 mm punches of the patches were kept on top of the monolayer of cells for 72 h. MTT assay was performed as per Pillai et al. [12]. To study the effect of degradation products of microneedle patches on cells, supernatants of patches incubated in SBF, were collected at different time intervals and incubated with HADF cells to assess their cytocompatibility. This experiment was conducted in accordance with ISO 10993-13 (part 3) [14].

*In vivo biocompatibility*

To assess the penetration of skin by the microneedle patch, C57BL/6 female mice were used (Ethical committee approval no. 05/2020). Five animals were used for this study: two for dissolving microneedle patches, two for hydrogel patches, and one as untreated control. Dorsal surface of the animal was shaved and two microneedle patches on opposite sides of the skin were inserted using fingers. At the end of day 7, animals were euthanized and their skin was collected. These skin samples were freshly subjected to cryo-microtome cutting for imaging with a fluorescence microscope (IX83, Olyumpus) for assessment of penetration and release of rhodamine dye into the skin. Samples were then stained with hematoxylin and eosin (H&E) as per the protocol given in Saha et al [15]. The extracted skin was also used for assessment of microneedle penetration using SEM after fixation.

*Statistical analysis*

All experiments were performed in triplicates and represented as mean ± standard deviation. Statistical analyses were performed using a one-way ANOVA with Tukey's test using GraphPad Prism and $p \leq 0.05$ was considered significant.

## Method validation

*Microneedle design and direct laser writing*

The dimensions of the microneedle array are shown in Table 1 . A 3 × 3 microneedle array design was made in Solidworks and laser written using Nanoscribe Photonic Professional GT (Germany). Fig. 1a shows the microneedle design used for 2PP, which took 3 h for the entire structure to be fabricated.

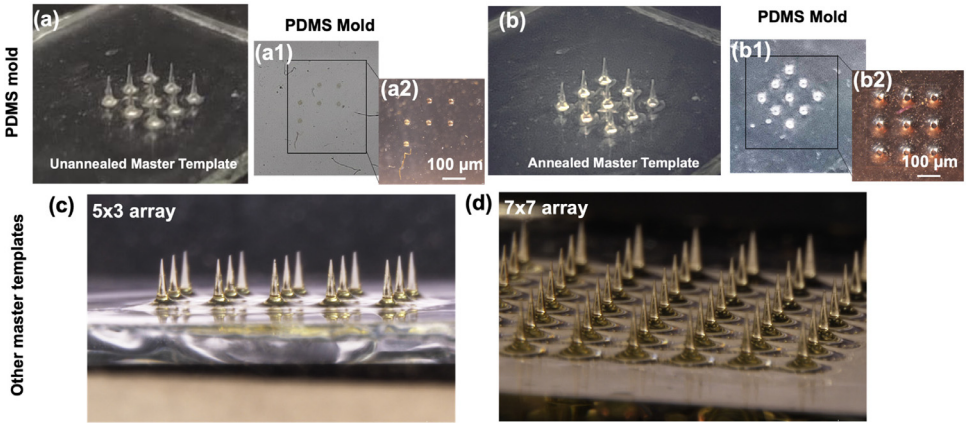


**Fig. 2.** Digital micrographs of (a) an unannealed template and its (a1) PDMS mold; (a2) Stereomicroscopic image of the PDMS mold; Digital micrographs of (b) an annealed master template and its (b1) PDMS mold; (b2) Stereomicroscopic image of the PDMS mold. Other laser written master templates of (c) 5 × 3 array and (d) 7 × 7 array.

*Annealed master template shows better PDMS peel-off*

The microneedle master template was spin-coated with resin and annealed at a high temperature. Stereomicroscopic (Fig. 1b and c) and SEM (Fig. 1d and e) images of the annealed (Fig. 1b-e) and the unannealed (Fig. 1f-i) templates. SEM images of the annealed template showed a uniform coating of the resin on the surface of the microneedles (Fig. 1h and i). This technique also provides additional strength to the microneedles for casting PDMS molds. The entire process for the fabrication of annealed and unannealed master templates is given in supporting information 1. PDMS molds casted from the unannealed (Fig. 2a) and annealed (Fig. 2b) templates showed the annealed templates to be sturdy enough for easy PDMS peel off enabling its multiple reuse (Figs. 2a1-a2). In case of unannealed template, needles were displaced, and molds were also not formed properly as needles got stuck onto the PDMS during casting and curing (Figs. 2b1-b2). To demonstrate the robustness of annealed templates, 5 × 3 (Fig. 2c) and 7 × 7 (Fig. 2d) arrays of microneedle templates were fabricated using this technique.

*Characterization of PVA microneedle patches*

PVA was used as a polymer for the development of microneedle patches. D-PVA and H-PVA microneedles were fabricated with and without the incorporation of rhodamine, which was used as a model drug. Fig. 3a shows the steps involving PDMS casting from the template and development of PVA polymer microneedle patches from the PDMS mold with (and without) crosslinker. Surface morphology and fluorescence of rhodamine-incorporated polymer microneedles can be seen in the SEM (Fig. 3b-c) and confocal images (Fig. 3d), respectively.

PVA is a non-toxic biomaterial widely used for fabrication of hydrogel microneedles. H-PVA microneedle patches (Fig. 3e) exhibit high swelling attributed to their hydrogel properties (Fig. 3f and g). The release profile of rhodamine (RD) from H-PVA-RD patches was studied for 12 days in PBS and it was found that 80.8 ± 1.9% of rhodamine was released at the end of the study (Fig. 4a). Degradation profiles of H-PVA and H-PVA-RD patches in SBF showed a weight loss of 30% at the end of 30 days (Fig. 4b). The compression test of RD-incorporated microneedle array performed as shown in the schematic of Fig. 4 reveals that after compression only the needle tip gets broken due to stress as depicted by the SEM image (Fig. 4d). H-PVA-RD exhibits higher compressive strength when compared to the un-crosslinked D-PVA-RD (Fig. 4e).

Fig. 5a shows complete degradation of the microneedle by day 24. Agar was used to simulate in vivo degradation wherein microneedle deformation at various time intervals was imaged stereo microscopically to assess morphological changes of the microneedle due to degradation in SBF. For the D-PVA microneedle patches fabricated without a cross-linker, the dissolving time was 17 m (Fig. 5b).

*Effect of microneedle shape on its stress profile and displacement profile of human skin*

The skin was modelled as a cylinder depicting various layers of skin (stratum corneum, epidermis and dermis) along its length (Fig. 6a). COMSOL was used to simulate microneedle penetration into human skin and a force of 5 N was applied to the needles of various shapes. von Mises stress profile of individual needles was assessed and the influence of needle shape on skin penetration was simulated. Stress profiles for cylindrical (Fig. 6b) and pyramidal (Fig. 6c) microneedles were found to be similar while the serrated microneedle showed highest stress ($3.3 \times 10^6$ N/m$^2$) as seen in Fig. 4d. Further, stress exhibited in microneedle array (4.89 N/m$^2$) was found to be lower that than that of its corresponding single cylindrical needle due to distribution of force across multiple microneedles (Fig. 6e). Skin displacement was found to vary depending on the needle shape as well. Lowest skin displacement was seen when a serrated needle (1 µm) penetrated in the human skin while maximum displacement was observed in case of a pyramidal

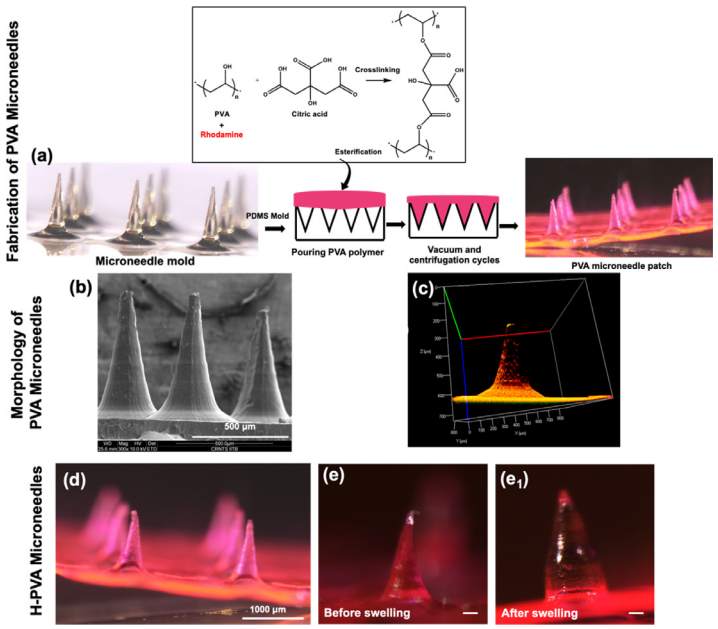


**Fig. 3.** (a) Steps for fabrication of PVA microneedle patch; SEM images of (b) 3 × 3 array and (c) single needle of PVA microneedle patch; (d) Confocal image of rhodamine incorporated PVA microneedle. Stereomicroscopic images of (e) H-PVA patch and single microneedle (f) before and (g) after swelling.

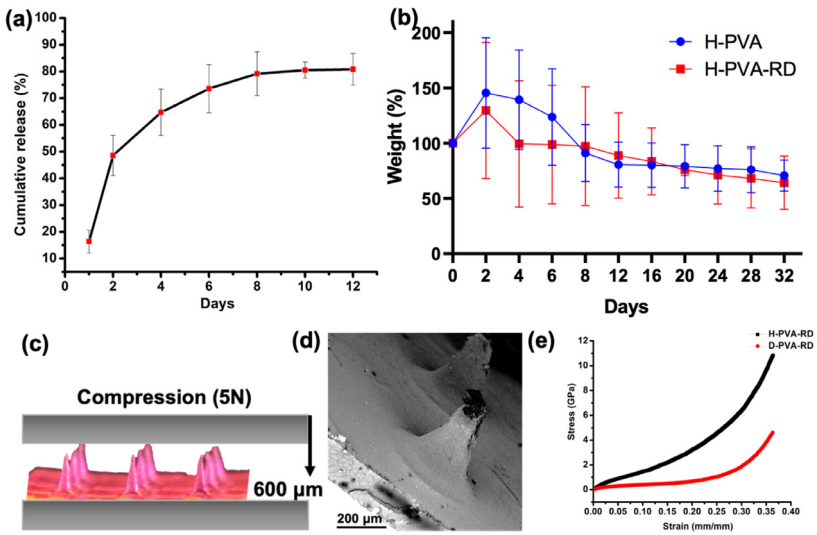


**Fig. 4.** Characterization of microneedles. (a) Cumulative release (%) of rhodamine from H-PVA microneedle patch; (b) Degradation profile of H-PVA microneedle patches in SBF upto 32 days; (c) Schematic showing compression test performed for microneedle array; (f) SEM image of microneedle after compression; (d) Stress vs. strain profile of H-PVA- RD and D-PVA-RD microneedle arrays. Data are shown as mean ± s.d. ($p \leq 0.05$).

needle (7.94 µm) as seen in Fig. 6f - h. Skin displacement was substantially more for microneedle array (14.6 µm) as compared to its corresponding single cylindrical needle

The microneedle tip was most affected by the penetration into the skin, as seen by the stress profile and SEM image of the microneedle following compression test. This study also provides evidence for the capability of the developed microneedles to penetrate human skin.

*Microneedle patches and their degradation products are cytocompatible*

In vitro cytocompatibility assessment for the microneedle patches was performed using three different methodologies, namely, hemocompatibility and cell viability using direct contact and degraded products of PVA microneedle patches (Fig. 7a). Biomaterials

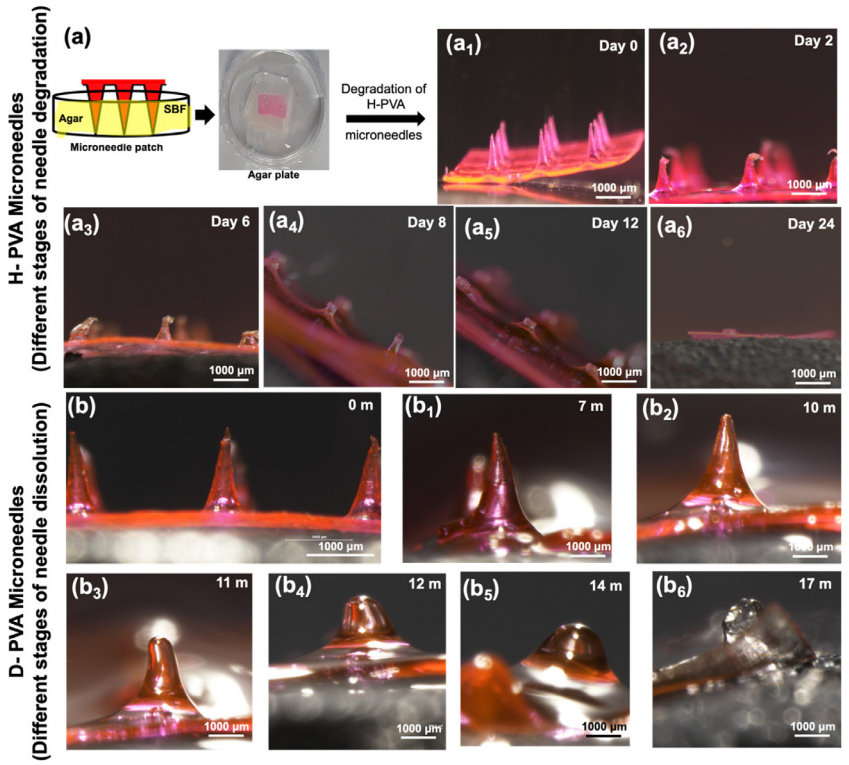


**Fig. 5.** Stereo-micrographs of various stages of (a) Degradation of an H-PVA hydrogel microneedle and (b) Dissolution of a dissolving D-PVA microneedle patch.

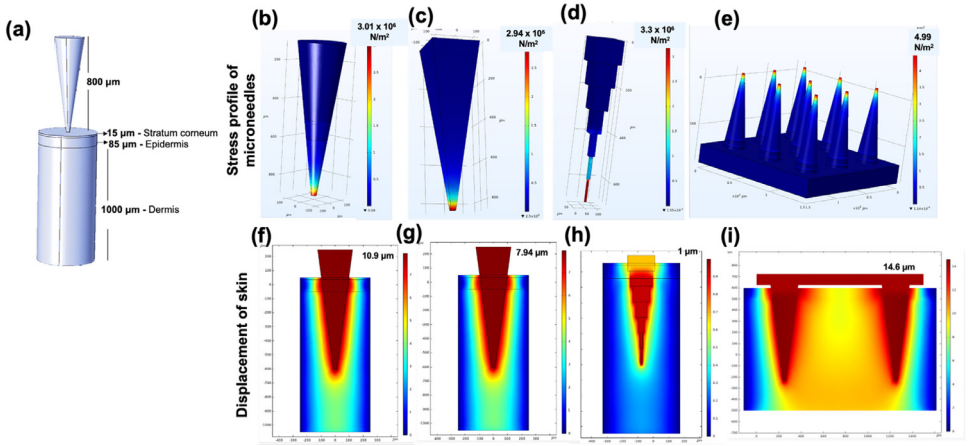


**Fig. 6.** Penetration of microneedle into human skin simulating stress. (a) Model representing penetration of microneedle into human skin; Stress profile of (b) cylindrical, (c) pyramidal, (d) serrated microneedle and (e) array of cylindrical microneedles inserted into human skin; Displacement profile of human skin upon penetration of (f) cylindrical, (g) pyramidal, (h) serrated microneedle and (e) array of cylindrical microneedles.

with a hemolytic index greater than 5% are considered non-hemocompatible as per ASTM F756-00 (2000) standard. Hemolysis percentage was found to be less than 2% (non-hemolytic) in the absence of RD in the patches with and without crosslinking, while incorporation of RD increased it to above 2%, making them slightly hemolytic (Fig. 7b). This may be due to a high dosage of RD in the patch. In vitro cytocompatibility of PVA patches was assessed using MTT assay. For the direct contact assay, patches were kept directly on an HADF monolayer for 72 h after which MTT assay was performed. All patches, with and without RD, gave a cell viability of ~90%. To assess the cytotoxicity due to degradation products of the patches, samples were incubated in SBF and supernatants containing the degraded products of patches were collected at different time intervals. These samples collected over 32 days were subjected to MTT assay and showed similar cytocompatibility.

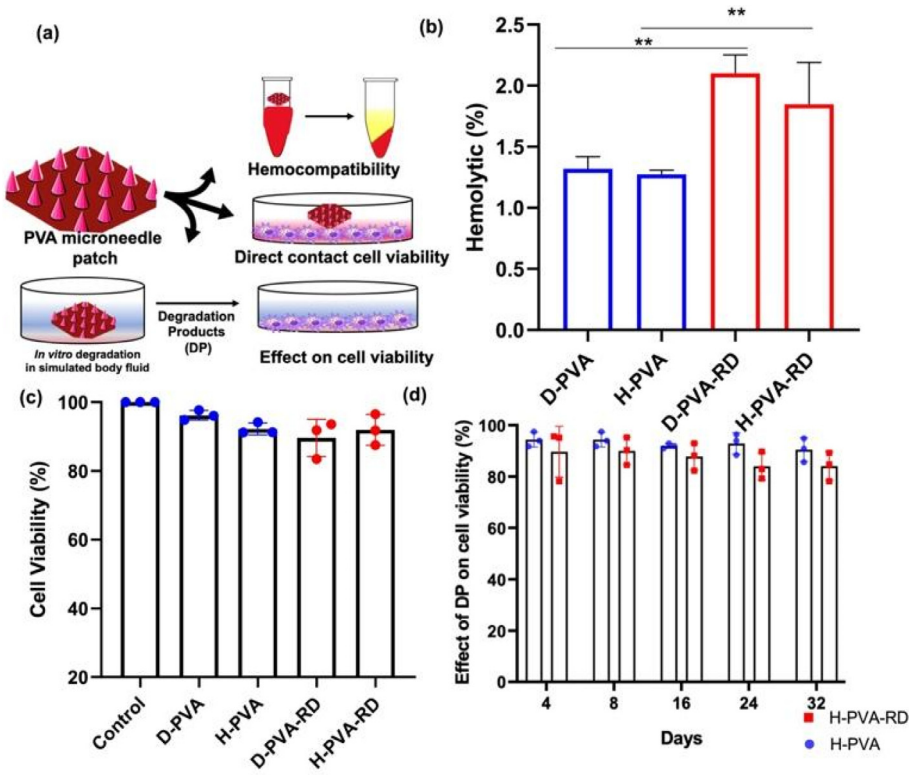


**Fig. 7.** (a) Different methodologies used for in vitro cytocompatibility assessment of microneedle patches; (b) Hemolysis (%); (c) Direct contact cell viability, and (d) Effect of degraded products of PVA microneedle patches on cell viability evaluated using MTT assay. Data are shown as mean ± s.d. ($p \leq 0.05$).

*Microneedles can effectively penetrate the skin of mice*

In vivo biocompatibility assessment of microneedle patches (D-PVA-RD and H-PVA-RD) was performed in C57BL/6 mice (Fig. 8a and b). At the end of day 7, patches were removed and skin was excised followed by imaging via fluorescence (due to RD) or bright field microscopy after H&E staining. There was no visible sign of sensitization or irritation on the skin where the patches were placed. SEM image of skin indicated microneedle puncture mark confirming its penetration (Fig. 8c). Fluorescence images validated the release of RD into the skin in both cases and showed a clear demarcation of the epidermis and dermis (Fig. 8d and e). H&E images also showed clear anatomical demarcation of the dermal layers of skin similar to control (Fig. 8f-h). In D-PVA patches, burst release of RD likely caused some immunogenic effects leading to immune cell infiltration (Fig. 8f). This result is in accordance with the in vitro hemocompatibility observed for high dosage of RD, as discussed earlier. However, in case of H-PVA patches, no immune cell infiltration was observed and patches were found to be biocompatible (Fig. 8g). Fig. 8h showing an H&E-stained image of untreated skin of mice showed a similar anatomical profile of the dermal layers.

## Discussion

Recently, transdermal drug delivery has gained a lot of attention for various diseases due to its semi-invasive mode. Drugs can be systemically administered via transdermal route which avoids elimination in the gastrointestinal tract or first-pass hepatic metabolism [16]. Microneedles are an array of micrometer-sized needles that puncture the outer layer of the skin to deliver drugs or biotherapeutics into the body. Microneedle-based delivery could be a commercially appealing product that improves patient compliance, especially for disease conditions that require repeated injections, such as hormone therapy, insulin delivery or even vaccination [1].

Most common methods for fabricating master templates for polymer microneedles include techniques such as stereolithography [17], electro discharge machining [18], 3D printing [19], which are either time-consuming, expensive or limited by poor mechanical properties, low aspect ratio, and precision (Table 2). Two-photon polymerization (2PP) enables fabrication of intricate micro-and nanoscale structures and outperforms other approaches in terms of geometric control, scalability, resolution, while also lowering the expenses associated with lithography and electro discharge-based techniques [20]. In this study, we have come up with a novel strategy for development of microneedle master templates using 2PP. A simple and quick (~ 5 min) annealing process was shown to be sufficient for fabrication of a robust master template of various microneedle arrays (3 × 3, 5 × 3 and 7 × 7) that could be reused multiple times (Fig. 1). The shortest needle length that can be printed using our optimized technique is 100 μm. Generally, 2PP written

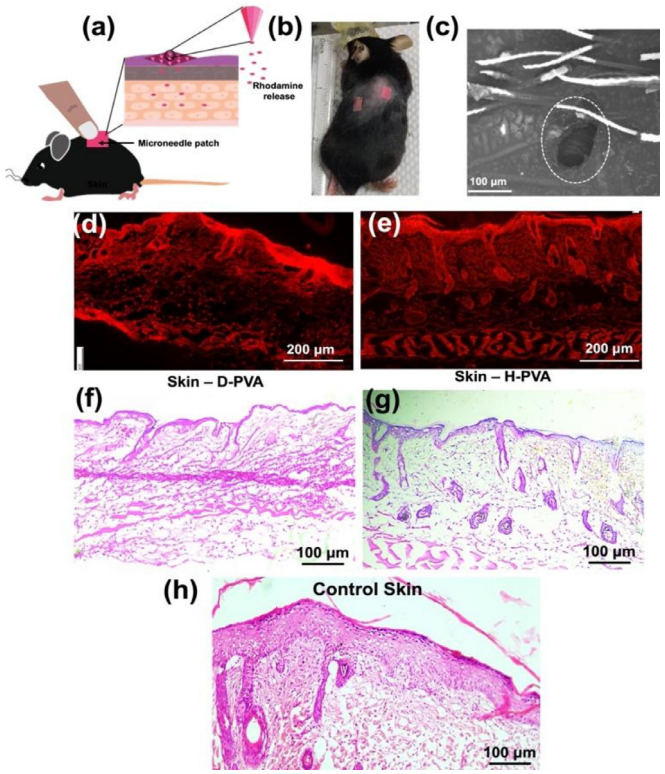


**Fig. 8.** In vivo biocompatibility assessment of microneedle patches performed in C57/BL6 mice. (a) Schematic showing microneedle insertion and subsequent rhodamine release in skin; (b) Digital micrograph showing insertion of PVA microneedle patch into the dorsal skin of mice; (c) SEM image showing marks from microneedle insertion into the skin; Fluorescence images of skin after removal of (d) D-PVA and (e) H-PVA patches. Histology of skin after removal of (d) D-PVA and (e) H-PVA patches; and of (h) Untreated control skin.

**Table 2**
Comparison of different printing techniques for microneedles.

| Technique | Advantages | Disadvantages | Ref |
|---|---|---|---|
| 3D printing | Cost effective | Low printing resolution | [4,5] |
| SLA | High printing resolution (~10 µm) | Requires additional processing | [17] |
| Electro discharge machining | Cost effective | Creating µm-sized structures is difficult | [18] |
| 2PP | High printing resolution (~200 nm) | Expensive equipment | [6] |

structures require 20-30 min of development using propylene glycol monomethyl ether acetate and isopropyl alcohol [6]. However, in this study, such post-processing is not required after direct laser writing. Further, in many laser-based fabrication techniques, other time-consuming post-processing steps are also involved before PDMS casting and curing. Hojatollah et al. [4] fabricated microneedle master templates by engraving them in an acrylic sheet using a $CO_2$ laser. These master templates were dried for 30 min and passivated overnight using trichloro (1H, 1H, 2H, 2H-perfluorooctyl) silane for subsequent fabrication of PDMS molds. Similar silane-based hazardous chemicals are used for passivation of templates for which appropriate safety measures need to be taken.

The annealed master molds in this investigation were not subjected to any development, passivation or post-processing procedures using hazardous chemicals, yet they could be reused more than 100 times. In this study, spin coating the photoresist on the fabricated template resulted in an additional thin layer of resin covering the surface and base of the microneedle. The additional layer aided in firmly anchoring the microneedle base and preventing it from falling off. Following the addition of the resin layer, a 1-minute spin coating ensures uniform resin deposition without compromising the fidelity of the microneedles (Fig. 1f -i). Acrylic resins are thermoset polymers, they can be hardened by a simple heat curing step [21]. The nanoscribe IPS resin contains photoinitiators, and heating promotes free-radical polymerization, resulting in more durable master templates. Subsequent annealing or heat treatment of these master templates at 190 °C considerably improved their strength and robustness. Fig. 2b shows that the resin coats the base of the needles, thereby giving them more strength and keeping them from falling off. This functionality, however, was not seen in the unannealed template (Fig. 2a). As a result, this approach aided in the non-adherence of PDMS to the templates allowing multiple replications.

PDMS negative molds were cast from these annealed master templates and different forms of PVA microneedles were fabricated, including the dissolving and hydrogel-forming microneedles. PVA was used as it is a biodegradable, non-toxic biomaterial that has already been cleared by the FDA for use in microneedle production [22]. Dissolving microneedles are designed with an ability to dissolve quickly after insertion, thereby, limiting the potential of infection transmission [23]. Many medications and biotherapeutics have been delivered transdermally and intradermally using dissolving microneedle patches such as insulin [24], ibuprofen sodium [25], metronidazole [26], erythropoietin [27], etc. Hydrogel-forming microneedle patches, which are made up of swellable biomaterials, are polymerized using appropriate crosslinkers. The swelling property of such microneedles makes them useful for transdermal delivery of drugs [28]. In this study, D-PVA microneedle patch showed dissolution after 17 m (Fig. 5b) while H-PVA microneedle patch showed good swelling properties (Fig. 3e) and a consistent release of the model drug RD up to 12 days (Fig. 4a). Complete degradation of the H-PVA microneedles was found to occur after 24 days. However, the backing layer of the microneedle array stayed intact. Microneedles showed suitable mechanical properties to penetrate human skin which was confirmed using simulation studies (Fig. 6). The findings confirm that the microneedles developed in this study are strong enough to penetrate human skin without breaking.

From the cytocompatibility analysis of PVA patches and their degradation products, cell viability of more than 70% (as shown in Fig 7c and d) indicates their nontoxic nature, as specified by ISO 10993-5:2009 [29]. The *in vivo* skin penetration studies for both forms of PVA microneedle patches were found to be similar and showed no signs of skin irritation or sensitization at the end of 7 days (Fig. 8). Fluorescence microscopy of extracted skin also showed RD release in both cases. However, the histology of skin around the dissolving needle patch demonstrated immune cell infiltration due to effects of high concentration of RD. The slow release of RD from the H-PVA microneedle patch showed no signs of immune cell infiltration in the skin.

One of the major drawbacks of this technique is that it cannot be used to anneal very small microneedles (less than 100 μm). Hollow microneedles cannot be printed using this technique because the temperature-based annealing technique hardens the entire microneedle.

## Conclusion

As new additive manufacturing technologies emerge, the potential for lowering the manufacturing time while maintaining high precision and reproducibility for fabrication of a highly durable microneedle template is becoming more apparent. Using 2PP, we were able to show a simple and cost-effective method for fabricating polymer microneedles. A high-quality, reusable and long-lasting master template (equivalent to metal-based master templates) can be fabricated with a simple annealing step. Master templates do not need to be subjected to time-consuming post-processing or surface-modification steps when using this method. Researchers will be able to avoid using hazardous chemical treatments while also accelerating the fabrication of microneedles with desired dimensions and shapes at high speeds and with exceptional precision better than any other microneedle fabrication technique.

## Ethics statements

Animal studies were performed after getting ethical committee approval from ACTREC, Mumbai (Approval number-05/2020). Animal experiments were strictly performed under CPCSEA (Committee for the Purpose of Control and Supervision of Experiments on Animals) guidelines.

## Declaration of Competing Interest

The authors declare that they have no known competing financial interests or personal relationships that could have appeared to influence the work reported in this paper.

## CRediT authorship contribution statement

**Mamatha M. Pillai:** Conceptualization, Methodology, Data curation, Writing – original draft. **Saranya Ajesh:** Conceptualization, Software. **Prakriti Tayalia:** Supervision, Software, Validation, Writing – review & editing.

## Data Availability

Data will be made available on request.

## Acknowledgments

We are grateful to the National Technical Textile Mission, Ministry of Textiles, Government of India, for funding this research (Grant No. 40924). We extend our acknowledgment to the 3D laser lithography central facility situated at IIT Bombay. We acknowledge Ms. Pooja Lokhande for preparing more than 100 PDMS molds from the master templates and Ms. Sarita Gurav for processing the samples for histology. The authors would like to thank the Department of Biotechnology (DBT) and IIT Bombay for providing an infrastructural facility for immuno-histochemistry (Grant No. BT/INF/22/SP23026/2017).

## Supplementary materials

Supplementary material associated with this article can be found, in the online version, at doi:10.1016/j.mex.2023.102025.

## References


[1] T. Waghule, G. Singhvi, S.K. Dubey, M.M. Pandey, G. Gupta, M. Singh, K. Dua, Microneedles: a smart approach and increasing potential for transdermal drug delivery system, Biomed. Pharmacother. 109 (2019) 1249–1258, doi:10.1016/J.BIOPHA.2018.10.078.

[2] J.H. Jung, S.G. Jin, Microneedle for transdermal drug delivery: current trends and fabrication, J. Pharm. Investig. 51 (2021) 503–517, doi:10.1007/S40005-021-00512-4/TABLES/2.

[3] Y. Chen, Y. Xian, A.J. Carrier, B. Youden, M. Servos, S. Cui, T. Luan, S. Lin, X. Zhang, A simple and cost-effective approach to fabricate tunable length polymeric microneedle patches for controllable transdermal drug delivery, RSC Adv. 10 (2020) 15541–15546, doi:10.1039/D0RA01382J.

[4] H.R. Nejad, A. Sadeqi, G. Kiaee, S. Sonkusale, Low-cost and cleanroom-free fabrication of microneedles, Microsystems Nanoeng. 41 (4) (2018) 1–7, doi:10.1038/micronano.2017.73.

[5] S.R. Dabbagh, M.R. Sarabi, R. Rahbarghazi, E. Sokullu, A.K. Yetisen, S. Tasoglu, 3D-printed microneedles in biomedical applications, IScience 24 (2021) 102012, doi:10.1016/J.ISCI.2020.102012.

[6] A.S. Cordeiro, I.A. Tekko, M.H. Jomaa, L. Vora, E. McAlister, F. Volpe-Zanutto, M. Nethery, P.T. Baine, N. Mitchell, D.W. McNeill, R.F. Donnelly, Two-Photon Polymerisation 3D printing of microneedle array templates with versatile designs: application in the development of polymeric drug delivery systems, Pharm. Res. 37 (2020) 1–15, doi:10.1007/S11095-020-02887-9/FIGURES/9.

[7] R.S.M. da Silva, R.C. Barbosa, C. dos Santos Chagas, E.B. da Silva, D. Feder, F.L.A. Fonseca, M.V.L. Fook, Development, preparation and characterization of chitosan, gelatin and heparin membranes for biomedical applications, SN Appl. Sci. 4 (2022) 1–9, doi:10.1007/S42452-021-04928-3/TABLES/1.

[8] G.K. Menon, G.W. Cleary, M.E. Lane, The structure and function of the stratum corneum, Int. J. Pharm. 435 (2012) 3–9, doi:10.1016/J.IJPHARM.2012.06.005.

[9] E.Z. Loizidou, N.A. Williams, D.A. Barrow, M.J. Eaton, J. McCrory, S.L. Evans, C.J. Allender, Structural characterisation and transdermal delivery studies on sugar microneedles: Experimental and finite element modelling analyses, Eur. J. Pharm. Biopharm. 89 (2015) 224–231, doi:10.1016/J.EJPB.2014.11.023.

[10] O. Olatunji, D.B. Das, M.J. Garland, L. Belaid, R.F. Donnelly, Influence of array interspacing on the force required for successful microneedle skin penetration: theoretical and practical approaches, J. Pharm. Sci. 102 (2013) 1209–1221, doi:10.1002/JPS.23439.

[11] U. Kanakaraj, T. Lhaden, V. Karthik Raj, Analysis of structural mechanics of solid microneedle using COMSOL software, ICIIECS 2015 - 2015 IEEE Int. Conf. Innov. Information, Embed. Commun. Syst (2015), doi:10.1109/ICIIECS.2015.7193243.

[12] M.M. Pillai, H. Dandia, R. Checker, S. Rokade, D. Sharma, P. Tayalia, Novel combination of bioactive agents in bilayered dermal patches provides superior wound healing, Nanomed. Nanotechnol. Biol. Med. 40 (2022) 102495, doi:10.1016/J.NANO.2021.102495.

[13] R. Deshpande, S. Shukla, A. Kale, N. Deshmukh, A. Nisal, P. Venugopalan, Silk Fibroin microparticle scaffold for use in bone void filling: safety and efficacy studies, ACS Biomater. Sci. Eng. 8 (2022) 1226–1238, doi:10.1021/ACSBIOMATERIALS.1C01103/SUPPL_FILE/AB1C01103_SI_001.PDF.

[14] ISO 10993-13:2010(en), Biological evaluation of medical devices — Part 13: identification and quantification of degradation products from polymeric medical devices, (n.d.). https://www.iso.org/obp/ui#iso:std:iso:10993:-13:ed-2:v1:en (accessed April 19, 2022).

[15] R. Saha, S. Patkar, D. Maniar, M.M. Pillai, P. Tayalia, A bilayered skin substitute developed using an eggshell membrane crosslinked gelatin–chitosan cryogel, Biomater. Sci. 9 (2021) 7921–7933, doi:10.1039/D1BM01194D.

[16] A.Z. Alkilani, M.T.C. McCrudden, R.F. Donnelly, Transdermal drug delivery: innovative pharmaceutical developments based on disruption of the barrier properties of the Stratum corneum, Pharmaceutics 7 (2015) 438–470 438-47072015, doi:10.3390/PHARMACEUTICS7040438.

[17] K.J. Krieger, N. Bertollo, M. Dangol, J.T. Sheridan, M.M. Lowery, E.D. O'Cearbhaill, Simple and customizable method for fabrication of high-aspect ratio microneedle molds using low-cost 3D printing, Microsystems Nanoeng. 51 (5) (2019) 1–14, doi:10.1038/s41378-019-0088-8.

[18] C.I. Shin, M. Kim, Y.C. Kim, Delivery of Niacinamide to the Skin Using Microneedle-Like Particles, Pharm 11 (11) (2019) 326 2019Page326, doi:10.3390/PHARMACEUTICS11070326.

[19] E. Mathew, G. Pitzanti, A.L. Gomes Dos Santos, D.A. Lamprou, Optimization of printing parameters for digital light processing 3d printing of hollow microneedle arrays, Pharm 13 (2021) 1837 2021Page131837, doi:10.3390/PHARMACEUTICS13111837.

[20] C. Liao, W. Anderson, F. Antaw, M. Trau, Two-Photon Nanolithography of Tailored Hollow three-dimensional Microdevices for Biosystems, ACS Omega 4 (2019) 1401–1409, doi:10.1021/ACSOMEGA.8B03164/SUPPL_FILE/AO8B03164_SI_004.AVI.

[21] J.J. Licari, D.W. Swanson, Adhesives Technology for Electronic Applications: Materials, Processing, Reliability, William Andrew, 2011 Jun 24.

[22] Na Xu, Manyue Zhang, Wenxin Xu, Guixia Ling, Jia Yu, Peng Zhang, Swellable PVA/PVP hydrogel microneedle patches for the extraction of interstitial skin fluid toward minimally invasive monitoring of blood glucose level, Analyst 147 (2022) 1478–1491, doi:10.1039/D1AN02288A.

[23] A.R.J. Hutton, H.L. Quinn, P.J. McCague, C. Jarrahian, A. Rein-Weston, P.S. Coffey, E. Gerth-Guyette, D. Zehrung, E. Larrañeta, R.F. Donnelly, Transdermal delivery of vitamin K using dissolving microneedles for the prevention of vitamin K deficiency bleeding, Int. J. Pharm. 541 (2018) 56–63, doi:10.1016/J.IJPHARM.2018.02.031.

[24] B. Demir, L. Rosselle, A. Voronova, Q. Pagneux, A. Quenon, V. Gmyr, D. Jary, N. Hennuyer, B. Staels, T. Hubert, A. Abderrahmani, V. Plaisance, V. Pawlowski, R. Boukherroub, S. Vignoud, S. Szunerits, Innovative transdermal delivery of insulin using gelatin methacrylate-based microneedle patches in mice and mini-pigs, Nanoscale Horizons 7 (2022) 174–184, doi:10.1039/D1NH00596K.

[25] Q.K. Anjani, A.H. Bin Sabri, E. Utomo, J. Domínguez-Robles, R.F. Donnelly, Elucidating the Impact of Surfactants on the Performance of Dissolving Microneedle Array Patches, Mol. Pharm. 19 (2022) 1191–1208, doi:10.1021/ACS.MOLPHARMACEUT.1C00988/ASSET/IMAGES/LARGE/MP1C00988_0014.JPEG.

[26] M.J. Garland, K. Migalska, T.M. Tuan-Mahmood, T. Raghu Raj Singh, R. Majithija, E. Caffarel-Salvador, C.M. McCrudden, H.O. McCarthy, A. David Woolfson, R.F. Donnelly, Influence of skin model on in vitro performance of drug-loaded soluble microneedle arrays, Int. J. Pharm. 434 (2012) 80–89, doi:10.1016/J.IJPHARM.2012.05.069.

[27] E.E. Peters, M. Ameri, X. Wang, Y.F. Maa, P.E. Daddona, Erythropoietin-coated ZP-microneedle transdermal system: Preclinical formulation, stability, and delivery, Pharm. Res. 29 (2012) 1618–1626, doi:10.1007/S11095-012-0674-Z/FIGURES/6.

[28] E.M. Migdadi, A.J. Courtenay, I.A. Tekko, M.T.C. McCrudden, M.C. Kearney, E. McAlister, H.O. McCarthy, R.F. Donnelly, Hydrogel-forming microneedles enhance transdermal delivery of metformin hydrochloride, J. Control. Release 285 (2018) 142–151, doi:10.1016/J.JCONREL.2018.07.009.

[29] ISO - ISO 10993-5:2009 - Biological evaluation of medical devices — Part 5: Tests for in vitro cytotoxicity, (n.d.). https://www.iso.org/standard/36406.html (accessed April 19, 2022).